## References


1 Bundy, F. B. and Strong, H. M., "Measurement of flame temperature, pressure and velocity," *Physical Measurements in Gas Dynamics and Combustion* (Princeton University Press, Princeton, N. J., 1954), Vol. IX, Sect. I, pp. 343–359.

2 Carlson, D. J., "Static temperature measurement in hot gas-particle flows," *Temperature, Its Measurement and Control in Science and Industry* (Reinhold Publishing Corp., New York, 1962), Vol. 3, Part II, pp. 535–550.

3 Gaydon, A. G. and Wolfhard, H. G., *Flames* (Chapman & Hall Ltd., London, 1960), 2nd ed., revised, Chap. IX, pp. 222–236.

4 Buttner, H., Rosenthal, I., and Agnew, W. G., "A study of flame temperatures as determined by the sodium-line reversal method in totally and partially colored flames," Project Squid Tech. Memo. PUR-27-M, Purdue Univ., Lafayette, Ind. (September 1, 1949).

5 Gaydon, A. F. and Hurle, I. R., "Measurements of times of vibrational relaxation and dissociation behind shock waves in $N_2$, $O_2$, air, CO, $CO_2$, and $H_2$," *Eighth Symposium (International) on Combustion* (Williams & Wilkins Co., Baltimore, Md., 1962), pp. 309–318.

6 White, W. B., Johnson, S. M., and Dantzig, G. B., "Chemical equilibrium in complex mixtures," J. Chem. Phys. **28**, 751–755 (1958).

7 Bulewicz, E. M. and Sugden, T. M., "The recombination of hydrogen atoms and hydroxyl radicals in hydrogen flame gases," Trans. Faraday Soc. **54**, 1855–1860 (1958).

8 Kaskan, W. E., "Hydroxyl concentrations in rich hydrogen-air flames held on porous burners," Combustion and Flame **2**, 229–243 (1958).

9 Kaskan, W. E., "The concentration of hydroxyl and of oxygen atoms in gases from lean hydrogen-air flames," Combustion and Flame **2**, 286–304 (1958).

10 Fenimore, C. P. and Jones, G. W., "Consumption of oxygen molecules in hydrocarbon flames chiefly by reaction with hydrogen atoms," J. Phys. Chem. **63**, 1834–1838 (1959).

11 Fenimore, C. P. and Jones, G. W., "Rate of reaction in hydrogen, nitrous oxide and in some other flames," J. Phys. Chem. **63**, 1154–1158 (1959).

12 Schott, G. L. and Kinsey, J. L., "Kinetic studies of OH radicals in shock waves, II: Induction times," J. Chem. Phys. **29**, 1177–1182 (1958).

13 Bulewicz, E. M., James, G. C., and Sugden, T. M., "Photometric investigations of alkali metals in hydrogen flame gases, II: The study of excess concentrations of hydrogen atoms in burnt gas mixtures," Proc. Roy. Soc. (London) **A235**, 89–106 (1956).

14 Duff, R. E., "Calculation of reaction profiles behind steady-state shock waves, I: Application to detonation waves," J. Chem. Phys. **28**, 1193–1197 (1958).

15 Westenberg, A. A. and Fristrom, R. M., "Methane-oxygen flame structure, IV: Chemical kinetic considerations," J. Phys. Chem. (to be published).

16 Kozlov, G. I., "On high temperature oxidation of methane," *Seventh Symposium (International) on Combustion* (Butterworths Scientific Publications, London, 1959), Part I, pp. 142–149.

17 Glick, H. S., "Shock tube studies of reaction kinetics of aliphatic hydrocarbons," *Seventh Symposium (International) on Combustion* (Butterworths Scientific Publications, London, 1959), Part I, pp. 98–107.

18 Bray, K. N. C., "Atomic recombination in a hypersonic wind-tunnel nozzle," J. Fluid Mech. **6**, 1–32 (1959).

19 Shapiro, A. H., *The Dynamics and Thermodynamics of Compressible Fluid Flow* (Ronald Press Co., New York, 1954), Vol. I., p. 228.

20 Byron, S., Baier, R., and Armour, W., "Application of the Bray criterion for prediction of atomic recombination effects in propulsion systems," Western States Section, Combustion Inst. Paper 62-6 (February 14, 1962).

21 Simmons, F. S., "Expansion of liquid-oxygen RP-1 combustion products in a rocket nozzle," ARS J. **30**, 193–194 (1960).

22 Simmons, F. S. and De Bell, A. G., "Spectral radiometry and two-path pyrometry of rocket exhaust jets," Rocketdyne Research Rept. RR 61-9 (May 1, 1961).

23 Ferriso, C. C., "The emission of hot $CO_2$ and $H_2O$ in small rocket-exit exhaust gases," *Eight Symposium (International) on Combustion* (Williams & Wilkins Co., Baltimore, Md., 1962), pp. 275–287.

24 Huff, V. N., Fortini, A., and Gordon, S., "Theoretical performance of JP-4 fuel and liquid oxygen as a rocket propellant, II: Equilibrium composition," NACA RM E56 D23 (September 7, 1956).

25 Carlson, D. J., "Experimental determination of thermal lag in gas-particle nozzle flows," ARS J. **32**, 1107–1109 (1962).


FEBRUARY 1963 AIAA JOURNAL VOL. 1, NO. 2

# Experiments with Two-Dimensional, Transversely Impinging Jets

DARSHAN S. DOSANJH* AND WILLIAM J. SHEERAN†
*Syracuse University, Syracuse, N.Y.*

**Experiments on the interaction of transversely impinging two-dimensional jet flows were performed in which a low pressure control jet flow interacted with a relatively high pressure power jet flow. The ratio of the control jet to the power jet supply chamber gauge stagnation pressure was adjusted at 0, 10, and 15%. Shadowgraphs of the power jet alone, as well as the corresponding interacting jet flows, were recorded to establish the nature of and changes in the shock structure. The jet flows were traversed by a pitot tube to record the pitot pressure distributions at various locations downstream of the power jet exit. It was discovered that with the addition of only a small percent control jet flow, the normal shock front of the highly underexpanded power jet flow changed to an oblique shock structure and, downstream of the previous location of the normal shock which appeared in the power jet flow alone, the maximum recovery stagnation pressures were proportionally much higher. The mechanism for this behavior of the normal shock is proposed. Possible practical importance of this behavior of interacting jet flows with reference to aerodynamic noise, supersonic diffuser losses, etc., is also pointed out. For the power jet flow alone it was found that by considering the actual jet boundaries as simply an extension of the actual nozzle, the average axial flow quantities, computed from the area-Mach number relation using the observed cross-sectional area of the jet flow, agreed quite favorably with the experimental results.**

## Introduction

DURING the last decade or two, scientific and engineering research on jet propelled high speed airplanes, missiles, and rockets has advanced at a phenomenally rapid pace. As a result of this accelerated emphasis and application of jet flows in numerous important developments, considerable basic jet flow investigations have been undertaken by a large number of research workers.[1] In comparison with the existing knowledge of the behavior of a single free jet flow, relatively less work has been done on the important basic aspects of the interaction of jet flows with external

Received by IAS May 7, 1962; revision received November 27, 1962. The authors appreciate the assistance of Thomas Weeks with the design of the experimental equipment. The senior author is pleased to acknowledge the time he spent in writing the paper while he was a Visiting Professor at the College of Aeronautics, Cranfield, England.

* Professor of Mechanical Engineering.
† Graduate Student, Mechanical Engineering Department.

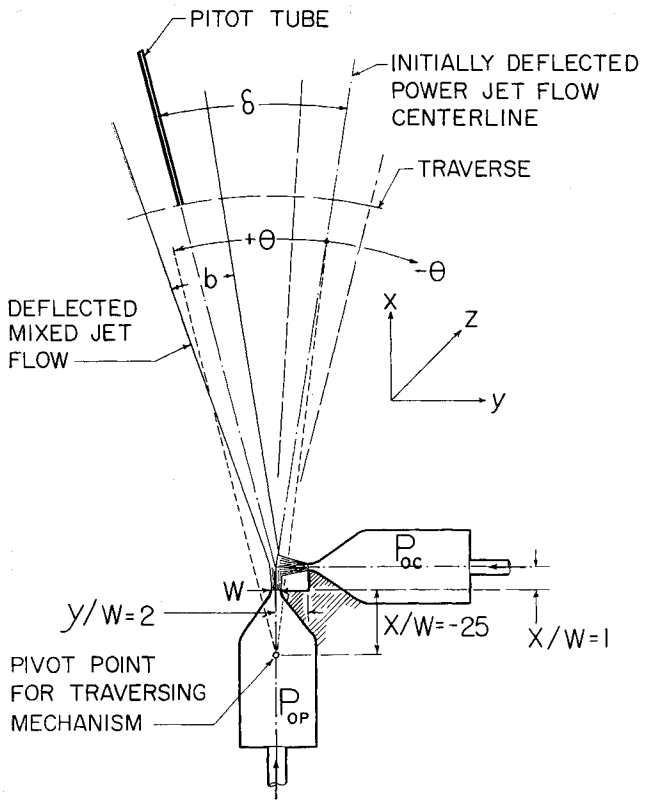


**Fig. 1 Illustration of interacting jets and important flow parameters**

flow fields. Such problems are important in the reduction of noise due to jet exhaust from high speed aircraft and rockets,[2] cooling of re-entry vehicles,[3] mixing of liquid propellants in rocket engines,[4] lift augmentation techniques,[5] and thrust vectoring.

In the field of the interaction of jet flows with external flow fields there has also been a recent development in pure pneumatic elements which has led to the design of fluid-operated control and computation systems which require no moving parts.[6] These pure pneumatic systems are rugged and reliable for simple operations and thus may be used to advantage in missile control and stability, or in servo-mechanisms and in environments where radiation or electromagnetic phenomena may interfere with the normal performance of electronic control and computing systems. Considerable amount of work in pure pneumatic systems has been done in Russia[7] and is briefly reported in Ref. 6. The basic subsystem of such pure pneumatic systems is the fluid amplifier in which a low-energy jet flow (input or control jet) is used to direct a high-energy fluid jet (output or power jet) to a receiver. The pressure gain of such a pneumatic amplifier may be defined as

$$\text{Gain} = \frac{\text{Incremental pressure delivered to the receiver or transducer}}{\text{Control jet pressure needed to direct the power jet to the receiver}}$$

$$= f(P_{0P}, P_{0C}, x/w, \delta, b, \ldots)$$

where $P_{0P}$ and $P_{0C}$ are the absolute stagnation pressures in the supply chambers of the power and control jets respectively; $x$ is the axial distance from the power jet exit; $w$ is the jet nozzle width—i.e., the small dimension of rectangular exit—$\delta$ is the angle of deflection; and $b$ is the width of the jet flow (Fig. 1).

To gain some insight into the basic behavior of such interacting jets, a preliminary investigation of transversely impinging jet flows was undertaken. Under an extended range

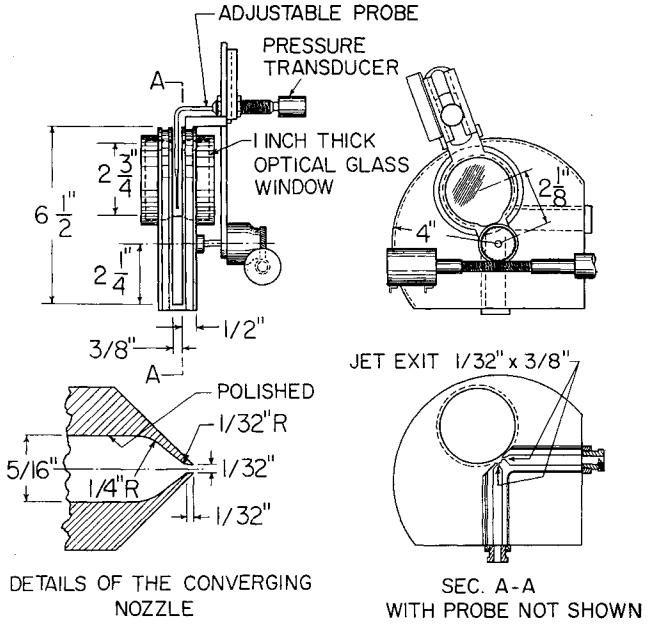


**Fig. 2 Jet arrangement and probe traversing mechanism**

of operating conditions, shadowgraphs of the interacting jet flows were recorded along with pitot tube traverses across the jet flows at various $x/w$ locations downstream of the power jet exit. From these, the characteristics of the interacting jet flows such as shock structure, deflection angles of the power jet, Coanda type deflection of the power jet, and pressure distributions were determined.[8] Only a few selected observations of general interest to fluid mechanics problems are presented here.

In most high-pressure ratio jet flows, shock structure is present. The exception would be the flow from a fully or correctly expanded nozzle designed specifically for a given operating pressure ratio. For relatively low-pressure ratios this shock system has a repetitive cellular structure;[1] however, at higher pressure ratios it is usually confined to one cell comprised of a normal shock and oblique intercepting shocks.[9,10] Since for these investigations only converging two dimensional nozzles were used over an extended range of pressure ratios, both the repetitive oblique shock waves present at low-pressure ratios and the system of intercepting and normal shock waves present in the jet flow at high-pressure ratios caused a considerable loss in stagnation pressure at locations downstream of such wave systems. Similar losses in available stagnation pressure are also present in high speed turbines, compressors, wind tunnels, diffusers, etc.

The observations reported here led to the discovery that when a relatively low-energy control jet flow is transversely impinged on a high-pressure ratio power jet flow, with the impingement point between the location of the normal shock and the jet exit, the wave structure in the high-pressure ratio power jet flow radically changes its nature in that the normal shock structure changes to a repetitive oblique or diamond shock structure. This change in shock structure results in comparatively much higher recovery jet flow stagnation pressures downstream of the axial position where the normal shock front appeared in the power jet flow alone. This phenomenon may have some important practical applications in fluid flow systems where, due to the necessity of high operating pressure ratios, the dissipative normal shock structure is unavoidable and at the same time recovering the maximum possible flow stagnation pressure is imperative or advantageous. The changing of the normal shock front in the flow to an oblique shock system may also have some important effects on the noise characteristics, especially screeching of high speed jets, and on the reduction of supersonic diffuser loss in high speed wind tunnels, etc.

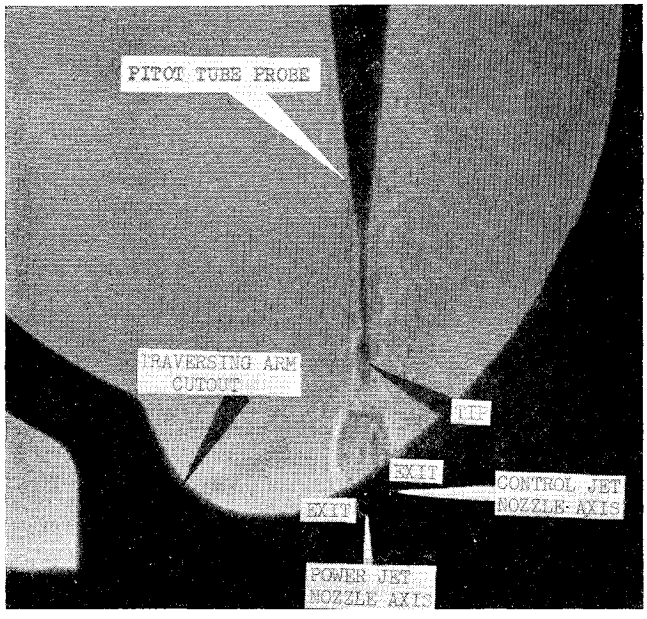


**Fig. 3 Shadowgraph of two-dimensional power jet flow ($P_{0P}$ = 214.49 psia, $P_a$ = 14.49 psia, probe tip at $x/w$ = 10, 0% control, ambient temperature = 71°F, and $T_{0P}$ = $T_{0C}$ = 71°F)**

## Experimental Facility and Procedure

The details of the test section, including the probe traversing mechanism, are shown in Fig. 2. The power jet settling or supply chamber gage stagnation pressure, $\bar{P}_{0P}$, and the control jet settling or supply chamber gage stagnation pressure, $\bar{P}_{0C}$, were measured in the large settling chambers of the power and control jets respectively; losses between these settling chambers and the smaller supply chambers just ahead of the exits were found to be negligible (maximum loss, ¼% of settling chamber pressure). The jet nozzle axes were arranged perpendicular to each other with the control jet nozzle axis being $x/w$ = 1 downstream from the power jet exit while the control jet exit was at $y/w$ = 2 from the power jet nozzle axis. No gap was provided between the power and control jet nozzles and the resulting asymmetric entrainment caused an initial deflection of the power jet flow toward the control jet nozzle (Fig. 1).

A curved pitot probe, the tip of which could be located at various axial distances downstream from the power jet exit, was employed to ensure minimum obstruction to the jet flow. The sensing portion of the probe was ⅜-in. long with 0.016-in. i.d. and a 0.0285-in. o.d. which gradually opened to a $\frac{3}{16}$-in. o.d. stem at the end of which a strain gage pressure transducer was mounted. The traversing mechanism pivoted about a point $x/w$ = −25 from the power jet exit (Fig. 1); the tip of the probe thus being directed at this point throughout the traverse. Using the electrical output signal from the calibrated pressure transducer, the jet-flow gage pitot pressures, $\bar{P}_{Tj}$, were found at various angular locations. The absolute pressure ratios $P_{Tj}/P_{0P}$ were calculated for the various angular locations in the jet flow and are plotted in Figs. 4 and 6 where $P_{Tj}$ = $\bar{P}_{Tj}$ + atmospheric pressure. The individual experimental points are shown at various percent controls; percent control being defined as the ratio of control jet to power jet supply chamber gage stagnation pressure, $\bar{P}_{0C}/\bar{P}_{0P}$.

## Discussion of Pitot Pressure Distributions

From the shadowgraph of the power jet flow alone—i.e., 0% control—it was established that with a power jet settling chamber pressure $P_{0P}$ = 214.5 psia, the shock structure in the jet flow was comprised of a combination of intercepting

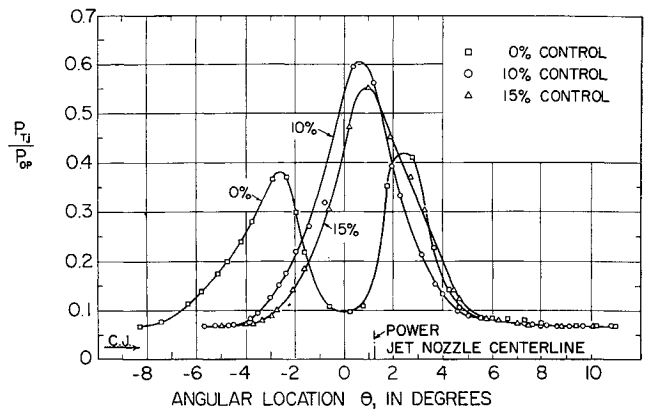


**Fig. 4 Pitot pressure variation with angular location, at various percent control ($P_{0P}$ = 214.46 psia, $P_a$ = 14.46 psia, probe tip at $x/w$ = 10, ambient temperature = 74°F, and $T_{0P}$ = $T_{0C}$ = 74°F)**

shocks and a normal shock, with the normal shock located at $x/w$ = 7.7 (Fig. 3). Therefore to record stagnation pressures downstream of the normal shock, the pitot tube tip was located at $x/w$ = 10. Since the Mach number of the flow downstream of the normal shock front was less than 1, no bow shock front appeared ahead of the tip of the pitot tube. A shadowgraph taken without the probe in the flow revealed that the presence of the pitot tube at $x/w$ = 10 did not noticeably influence the configuration of the shock structure.

For the power jet flow alone, at $x/w$ = 10 the plots of the pressure ratio $P_{Tj}/P_{0P}$ vs the angular location $\theta$ exhibited a low pressure region extending about one degree on either side of the center of the power jet flow (Fig. 4).‡ In this central region the ratio of the absolute pressure $P_{Tj}/P_{0P}$ was only equal to 0.098; obviously then the stagnation pressure loss through the main normal shock front in the jet flow was quite high. Higher pressure peaks, corresponding to the outer region of the jet flow between the intercepting shocks and the jet boundary, appeared on either side of the central region. This was due to the fact that the flow streamlines crossed the intercepting shocks at fairly small angles and thus the entropy rise and loss in stagnation pressure was relatively less severe than that through the main normal shock. The peak pressure ratio on the side toward the control jet (left-hand side of the plot) was equal to 0.382 and the peak pressure ratio on the far side was equal to 0.42.

With the addition of 10% control jet flow, the nature of the jet flow shock structure radically changed§ (Fig. 5) which introduced a corresponding radical change in the pitot pressure distribution (Fig. 4); a smooth Gaussian type pitot pressure distribution with no dip in the middle or peaks on the sides being the result. The recovery pitot pressure ratio corresponding to the center of the jet was equal to 0.605 which meant that by an addition of 10% control the recovered $P_{Tj}/P_{0P}$ in the center of the power jet flow jumped from 0.098 to 0.605. Therefore, the local centerline pitot pressure of the jet flow increased from 21.02 to 129.77 psia, which is a tremendous gain. After the normal shock structure collapsed with the addition of the control jet flow, the tip of the probe was in supersonic flow (Fig. 5) and therefore recorded a lower stagnation pressure behind its bow shock wave. This means that the increase in the actual jet stag-

‡ For discussion of the deflection of the power jet flow,[8] the angle $\theta$ given by traversing mechanism may be changed, from known geometry of the system, to the angle $\delta$ whose origin is referred to the point of intersection of the axes of the power and control nozzles (Fig. 1).

§ Subsequently it has been observed that the normal shock structure collapses even for 2% control.[11]

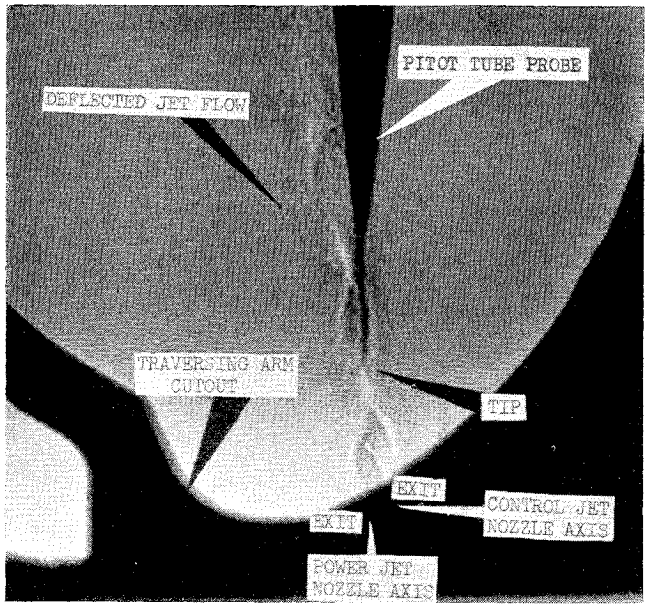


**Fig. 5 Shadowgraph of interacting two dimensional jet flows ($P_{0P}$ = 214.49 psia, $P_a$ = 14.49 psia, probe tip at $x/w$ = 10, 10% control, ambient temperature = 71°F, and $T_{0P} = T_{0C}$ = 71°F)**

nation pressure is even greater than that indicated by the pitot probe.

Additional traverses of the pitot pressure of the jet flow were taken for $P_{0P}$ = 214.5 psia with the probe at $x/w$ = 5 downstream of the power jet exit Since the normal shock in the power jet flow occurred at $x/w$ = 7.7, the probe tip was located where the central region of the expanded jet flow was supersonic, and thus as discussed earlier the pitot tube registered the local stagnation pressure behind its normal bow shock front. The location of the main normal shock front observed in the power jet flow alone did not seem to be affected by the presence of the pitot stem.

As in the $x/w$ = 10 case, the $P_{Tj}/P_{0P}$ vs $\theta$ plot at $x/w$ = 5 for 0% control, had a substantial pressure drop in the central region of the jet flow which was caused by the presence of the probe bow shock wave (Fig. 6). Higher pressure peaks corresponding to the outer region of the jet flow were again symmetrically located on either side of the central region; the stagnation pressure loss through the intercepting shocks being relatively less severe than that through the normal part of the probe bow shock wave. With the addition of 10% control jet flow the central region absolute pitot pressure ratio increased 82% and with 15% control it increased 115% over the 0% control value of 0.156.

## Proposed Mechanism

The normal shock may be assumed to occur at an axial location where the shock will attain sufficient strength to raise the local axial static pressure of the jet flow to the ambient atmospheric pressure. Since the control jet flow was impinged on the power jet flow upstream of the normal shock location, new velocity and static pressure conditions were imposed on the outer region flow which crossed the intercepting shock on the control jet side. To satisfy these conditions, the intercepting shock appeared to move inward towards the power jet center-plane, thereby reducing the extent of the inner flow region, i.e., the region bounded by the intercepting and normal shocks. Also, the relocated intercepting shock made larger wave-angles with the flow streamlines. This readjustment of the intercepting shock became more pronounced with increasing percent control until at 10% control the relocated intercepting shock appeared to extend across the central region of the power jet flow meeting the far-side

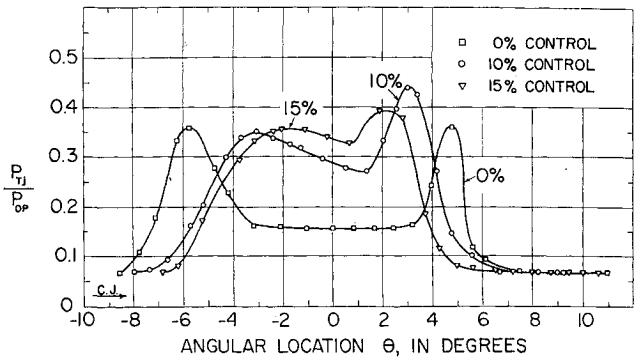


**Fig. 6 Pitot pressure variation with angular location, at various percent control ($P_{0P}$ = 214.53 psia, $P_a$ = 14.53 psia, probe tip at $x/w$ = 5, ambient temperature = 77°F, and $T_{0P} = T_{0C}$ = 77°F)**

intercepting shock at a downstream location of approximately $x/w$ = 4. An interface (slip surface) was formed in the outer region between the control jet flow and the power jet flow which crossed the relocated intercepting shock. Because of the density changes across it, this interface appears similar to an oblique shock in the shadowgraph (Fig. 5). Across the relocated intercepting shock the local low pressure of the inner flow increased to the ambient pressure in the outer region, thus eliminating the need for the normal shock. Since the intercepting shock was relocated closer to the power jet exit where the local Mach number was less than that just before the normal shock and since it was also oblique to the flow, the stagnation pressure losses across it were less than those across the normal shock. Because of the reduced extent of the first shock-cell, the interacted power jet flow expanded such that its lowest pressure was higher and its maximum Mach number was lower than for the power jet flow alone. Therefore this lower effective expansion pressure ratio resulted in the repetitive wave structure and the decreased spread of the interacted jet flow (Fig. 4). Similar changes in the normal shock structure were also observed in shadowgraphs taken with $P_{0P}$ = 314.5 psia.

## Analytical Interpretations

Some of the experimental observations of the pressure distribution in the power jet flow alone can be explained from the following simple analytical considerations.

The ratio of the stagnation pressure ahead of a normal shock, $P_{01}$, to the local stagnation pressure behind it, $P_{02}$, is given by

$$\frac{P_{01}}{P_{02}} = \left(\frac{2\gamma}{\gamma+1} M_1^2 - \frac{\gamma-1}{\gamma+1}\right)^{1/(\gamma-1)} \times \left(\frac{2+(\gamma-1)M_1^2}{(\gamma+1)M_1^2}\right)^{\gamma/(\gamma-1)} \quad (1)$$

This relation was applied to find the centerline Mach number at $x/w$ = 5 where a bow shock wave was present just ahead of the pitot tube tip. Considering that the jet flow expanded isentropically from the settling chamber to Mach number $M_1$ ahead of the normal part of bow shock, then $P_{01} = P_{0P}$ = 214.5 psia and the Mach number, $M_1$, of the flow at this location could be found from Eq. (1). At $x/w$ = 5 and $P_{0P}$ = 214.53 psia, $P_{02}$ = 33.1 psia was recovered in the central region of the jet flow (Fig. 6); thus $P_{02}/P_{01}$ = 0.154. Then from Eq. (1) the corresponding centerline Mach number, $M_1$, was found to be equal to 3.86 for $\gamma$ = 1.4.

The centerline pitot pressure at $x/w$ = 10 was measured to be 20.84 psia. In this case the pitot tube tip was in the region of subsonic flow downstream of the normal shock; therefore to compare the experimental pitot pressure with the expected one, it was necessary to know the strength of the main normal shock in the jet flow. By placing the tip

of the pitot tube just upstream of the main normal shock and measuring the local stagnation pressure behind its bow wave, it was determined from Eq. (1) that the Mach number just ahead of the main normal shock front was approximately 4.3. Considering isentropic jet flow expansion from the settling chamber to the upstream side of the main normal shock—i.e., $P_{01} = P_{0P} = 214.46$ psia—the value of the stagnation pressure on the downstream side of the main normal shock, $P_{02}$, was predicted to be 23.04 psia. As there is some decay in this jet centerline stagnation pressure in the subsonic flow region from the downstream side of the main normal shock located at $x/w = 7.7$ to the position of the probe tip at $x/w = 10$, the experimentally observed and the predicted stagnation pressure agreed well.

From these studies it was also found that the approximate average Mach numbers at axial positions upstream of the normal shock for the power jet flow alone could be calculated by simply assuming that the actual jet boundary was an extension of the sonic nozzle. The isentropic one-dimensional area-Mach number relation

$$\frac{A^*}{A_1} = M_1 \left( \frac{\gamma + 1}{2 + (\gamma - 1) M_1^2} \right)^{(\gamma+1)/2(\gamma-1)} \qquad (2)$$

($A^*$ being the nozzle exit area) was used to find the average $M_1$ where the local jet flow cross-sectional area $A_1$ was determined either directly from shadowgraphs or from the known radius of traverse and the full angular width of the jet flow as given by the $P_{Tj}/P_{0P}$ vs $\theta$ plot. The use of this area requires that the entropy rise (or total pressure loss) introduced by the intercepting shocks be negligible. For rough approximation this was considered to be the case because at the low nozzle-exit to ambient pressure ratio of 7.67, the expanded jet flow crossed relatively weak intercepting shock fronts at fairly small angles.

At $x/w = 5$, for 0% control, $A^*/A_1 = 0.12$ and thus from Eq. (2), $M_1 = 3.72$, as compared to 3.86 found earlier from experimental measurement. Using $M_1 = 3.72$ and $P_{01} = 214.53$ psia in Eq. (1), $P_{02}$ was found to be equal to 37.5 psia, as compared with the experimental value of 33.1 psia. This meant that the large loss in the local stagnation pressure, $P_{01}$, in the central region of the jet flow, due to the presence of the bow shock wave ahead of the probe tip, is predicted to be only about 2% lower than the experimental value.

An attempt was also made to calculate the local stagnation pressure expected at $x/w = 10$, with $P_{0P} = 214.46$ psia, at 0% control. Using the above procedure, the Mach Number just ahead of the main normal shock was calculated to be 4.03 as against 4.3 derived earlier from experimental measurement. Using $M_1 = 4.03$ and $P_{01} = 214.46$ in Eq. (1), $P_{02}$ at $x/w = 7.7$ was predicted to be equal to 29.02 psia. The decay of the centerline stagnation pressure between the downstream side of the normal shock and the pitot tube tip located at $x/w = 10$ should be taken into account before the predicted $P_{02}$ can be compared with the experimentally observed value of 20.84 psia. The value of this decay was not known. However, even assuming no decay, the predicted loss in the maximum available jet flow stagnation pressure of 214.46 psia is only about 5% lower than that recorded experimentally. It is surprising that these simple assumptions lead to such close agreement. For jets operated at higher pressure ratios, however, the disagreement may be more pronounced.[11] In that case the more exact, though tedious, method of characteristics could be used.

## References


[1] Pai, S. I., *Fluid Dynamics of Jets* (Van Nostrand Company, Inc., New York, 1954).

[2] Coles, W. E. and Mihaloen, J. A., "Turbojet engine noise reduction with mixing nozzle-ejector combination," NACA TN 4317 (1958).

[3] Warren, C. H. E., "An experimental investigation of the effect of ejecting a coolant gas at the nose of a blunt body," GALCIT Rept. Memo. no. 17 (Dec. 1958).

[4] Eleverum, G., Jr. and Morey, T., "Criteria for optimum mixture-ratio distribution using several types of impinging-steam injector elements," Memo. no. 30-5, Jet Propulsion Lab., C.I.T., Pasadena, Calif. (Feb. 1959).

[5] Spence, D. A., "The lift on a thin aerofoil with jet augmented flaps," Aeronaut. Quart. **IX**, Pt. 3 (1958).

[6] Bowles, R. E., Hinshelwood, G. D., Horton, B. M., and Palmisano, R. R., "Pure pneumatic systems," R-310-50-12, Diamond Ordnance Fuze Labs., Ordnance Corps, U. S. Army, Washington, D. C. (Dec. 1959).

[7] Zalmanzon, L. A. and Semikova, A. I., "Investigations of the characteristics of pneumatic jet elements," Automatika i Telemekhanica **20**, no. 4 (April 1959).

[8] Dosanjh, D. S., "Interaction of confined two-dimensional transversely impinging jets," DSL R-65, Syracuse Univ. Res. Corp., submitted to Diamond Ordnance Fuze Laboratories, Washington, D. C. (Aug. 1961).

[9] Adamson, T., Jr. and Nicholls, J., "On the structure of jets from highly underexpanded nozzles into still air," J. Aero/Space Sci. **26**, 16–24 (1959).

[10] Love, E. S., Grigsby, C. E., Lee, L. P., and Woodling, W. P., "Experimental and theoretical studies of axisymmetric free jets," NASA TR R-6 (1959).

[11] Dosanjh, D. S. and Sheeran, W. J., "Interaction of transversely impinging jets," Proceedings of the Fluid Amplification Symposium, Diamond Ordnance Fuze Laboratories, Washington, D. C. (Oct. 1962).


[11] The authors appreciate the comments of Prof. T. C. Adamson on this point.